A New Power Series Solution Approach to Solving Electrically Large Complex Electromagnetic Scattering Problems

Sadasiva M. Rao and Michael S. Kluskens

Naval Research Laboratory
Washington DC 20375, USA.

Abstract – In this work, we present a new power series solution procedure to obtain induced currents and scattered fields on a large conducting body due to a plane wave incidence. The procedure follows standard method of moments approach yet is applicable to electrically large problems. The first step involves approximating the given structure via standard geometrical discretization and defining the conventional basis functions to approximate the induced current. The next step involves gathering the total number of basis functions into a small number of groups thereby casting the moment matrix into a collection of submatrices representing self and mutual interaction between the groups. Next, the procedure involves eliminating the interaction of two immediate neighbors on any selected group. This process results in a diagonally-dominant moment matrix assuming the group size is sufficiently large. Also the procedure sets the matrix blocks residing on either side of the diagonal block to zero. The new matrix equation can be solved in many ways efficiently. However, this work proposes using power series approach to obtain accurate solution results. The present approach is simple, efficient, highly amenable for parallel processing, and retains all the advantages of conventional method of moments scheme. Several numerical examples are presented to validate the numerical method.

Index Terms – Electromagnetic fields, Integral equations, Method of moments, Numerical methods.

I. INTRODUCTION

The method of moments (MOM) solution technique [1] - [5], one of the most popular methods for solving electromagnetic scattering and radiation problems, is limited by excessive computational and memory requirements if applied in a conventional way to electrically large scattering problems. The objective of the present work is to overcome this MOM limitation and apply the procedure to truly complex and practical problems.

There exist several new algorithms which seem to overcome the limitation of MOM. Notable among them are: a) recently developed fast multipole method (FMM) using matrix approximations to reduce the memory and computational time requirements [6], and adaptive cross approximation (ACA) method [7]. However, both are approximate methods and the accuracy of the overall solution depends on the level approximation and may become expensive when high accuracy solutions are desired. Further, FMM also sacrifices one of the most important advantages of MOM, i.e., the ability to handle multiple right hand sides in a simple manner.

In a recent work, Killian et al. [8] have proposed a method to solve the electromagnetic scattering by electrically large conducting bodies via MOM. The procedure involves dividing the body into relatively large subsections and, using some simple numerical steps, the mutual-coupling between a given subsection and related nearby subsections is transformed into self-coupling. The resulting current distribution, sufficiently accurate on major part of the body, is later improved to the desired degree of accuracy on the whole body by using an iterative scheme. Although the central idea of this procedure is quite novel, the numerical procedure presented is cumbersome, inefficient, and not easily applicable to complex practical problems.

The present work adopts the central idea of [8]. However, the new procedure presented here completely modifies the numerical scheme using several important steps. The present procedure is more efficient by several orders, very stable, accurate and easily and efficiently applicable to complex practical problems. The modifications and resulting novelty of the new procedure are enumerated in the following:

- For the new procedure to work well, a diagonally-strong, preferably diagonally-

Submitted On: February 5, 2016
Accepted On: March 14, 2016

dominant, moment matrix is required to begin with. A simple scheme is devised in this work to obtain such a moment matrix for complex two and three-dimensional objects. The scheme involves renumbering the basis functions using a distance criterion and adopting Galerkin scheme wherein the basis functions are also used as testing functions. We note that this step is the most important modification as discussed further.

- The cumbersome search process for the near-field basis functions, necessary for the algorithm presented in [8] but made the procedure inefficient, is totally eliminated. This step makes the algorithm not only fast but also highly suitable for parallel processing, and much more user-friendly.

- The new method involves dividing the total number of basis functions into groups of equal size. The equal size criterion makes the algorithm much more simple and efficient than [8].

- The mathematical steps in the new algorithm are simple and represent mere algebraic manipulations. Hence, any standard MOM algorithm can be easily converted into adopting the procedure presented in this work.

In the following section, we present the detailed mathematical steps describing the algorithm. In Section III, we present several important empirical guidelines to apply the procedure successfully. In Section IV, we present several numerical results to test the validity of the technique. Finally, Section V discusses important conclusions along with possible improvements and future work to be undertaken in this area.

II. NUMERICAL SOLUTION PROCEDURE

Consider an electrically large perfectly electric conductor (PEC) problem given by,

$$\boldsymbol{L}\boldsymbol{I} = \boldsymbol{V}, \tag{1}$$

where $\boldsymbol{L}$, $\boldsymbol{I}$, and $\boldsymbol{V}$, are the integral equation operator, unknown vector describing the induced currents, and known excitation vector representing the incident field, respectively. The integral equation operator adopted in this work is the combined field operator given by,

$$\boldsymbol{Z}_{CFIE} = \gamma \boldsymbol{Z}_{EFIE} + \eta(1-\gamma)\boldsymbol{Z}_{MFIE}, \tag{2}$$

$$\boldsymbol{Y}_{CFIE} = \gamma \boldsymbol{Y}_{EFIE} + \eta(1-\gamma)\boldsymbol{Y}_{MFIE}, \tag{3}$$

where $0 \leq \gamma \leq 1$ is a constant depending on the problem and η is the impedance of the medium. For open body problems, we let $\gamma = 1$ and for closed bodies γ is typically 0.5. In Eq. (3), the quantities $\boldsymbol{Z}_{EFIE}$, $\boldsymbol{Z}_{MFIE}$ represent $N \times N$ matrices and $\boldsymbol{Y}_{EFIE}$ and $\boldsymbol{Y}_{MFIE}$ represent $N \times 1$ column actors, respectively, where N represents the number of the unknowns in the MOM scheme. Further, these quantities are obtained by applying the MOM procedure to the integral equations given by,

$$\boldsymbol{E}^i_{tan}(\boldsymbol{r}) + \boldsymbol{E}^s_{tan}(\boldsymbol{r}) = 0, \ \boldsymbol{r} \in S_c \tag{4}$$

and

$$\boldsymbol{J}(\boldsymbol{r}) = \hat{n} \times (\boldsymbol{H}^i(\boldsymbol{r}) + \boldsymbol{H}^s(\boldsymbol{r})), \ \boldsymbol{r} \in S_c \tag{5}$$

where $(\boldsymbol{E}^i, \boldsymbol{H}^i)$ and $(\boldsymbol{E}^s, \boldsymbol{H}^s)$ are the incident and scattered fields, respectively, $\boldsymbol{J}$ is the induced current, S_c is the conductor surface, $\hat{n}$ represents the unique outward normal to S_c, and the subscript "tan" represents the tangential component.

To begin the numerical procedure we follow the conventional MOM and approximate the current distribution on the given electrically large perfectly conducting (PEC) structure using standard subdomain functions. Thus, for two dimensional problems we use linear segments and define pulse basis functions [3]; whereas, for three dimensional problems, we use planar triangular subsections and define Rao-Wilton-Glisson (RWG) basis functions [9] for the solution of electromagnetic scattering problem.

Next, we order the basis functions using a distance criterion measured from a reference point, either from one end of the scatterer or from a convenient point on the scatterer. This arrangement makes the first basis function closest to the reference point and the last one the farthest. This is a very important step in the new algorithm which eventually eliminates the cumbersome search procedure for nearest neighbors adopted in [8]. We also note that the actual location of the reference point is of no importance and does not affect the final results in any way.

Using the basis functions also as testing functions and following the standard method of moments procedure, the operator equation can be transformed into a matrix equation given by,

$$\boldsymbol{Z}\boldsymbol{X} = \boldsymbol{Y}. \tag{6}$$

where $\boldsymbol{Z} = \boldsymbol{Z}_{CFIE}$ is a $N \times N$ matrix and $\boldsymbol{X}$ and $\boldsymbol{Y} = \boldsymbol{Y}_{CFIE}$ are the unknown and known column vectors of dimension N, respectively. Note that, because of the re-ordering of the basis functions as mentioned before, in each row of the $\boldsymbol{Z}$-matrix, the diagonal element is the largest element magnitude-wise and off-diagonal elements progressively decrease away from the diagonal element.

Next, we assemble the total number of basis functions into groups with each group containing

a fixed number of micro-basis functions. Here, we note that each group corresponds to a block of elements in the global MOM matrix. Again, this step is in contrast to the procedure adopted in [8] where each group may have different size making the bookkeeping cumbersome.

Let us divide the N basis functions into P groups, with $M = N/P$ elements in each group. The $\boldsymbol{Z}$-matrix may be written as:

$$\boldsymbol{Z} = \begin{bmatrix} \boldsymbol{Z}_{11} & \boldsymbol{Z}_{12} & \boldsymbol{Z}_{13} & \cdots & \boldsymbol{Z}_{1P} \\ \boldsymbol{Z}_{21} & \boldsymbol{Z}_{22} & \boldsymbol{Z}_{23} & \cdots & \boldsymbol{Z}_{2P} \\ \boldsymbol{Z}_{31} & \boldsymbol{Z}_{32} & \boldsymbol{Z}_{33} & \cdots & \boldsymbol{Z}_{3P} \\ \vdots & \vdots & \vdots & \vdots & \vdots \\ \boldsymbol{Z}_{P1} & \boldsymbol{Z}_{P2} & \boldsymbol{Z}_{P3} & \cdots & \boldsymbol{Z}_{PP} \end{bmatrix}, \quad (7)$$

where each $\boldsymbol{Z}_{ij}, i = 1, 2, \cdots, P, j = 1, 2, \cdots, P$ represents a submatrix of $M \times M$. In a similar manner, we can express the column vector $\boldsymbol{Y}$ as:

$$\boldsymbol{Y} = \left[\boldsymbol{Y}_1, \boldsymbol{Y}_2, \boldsymbol{Y}_3, \cdots, \boldsymbol{Y}_P\right]^T, \quad (8)$$

where the superscript "T" represents the transpose.

Next, we transform the Eq. (6) to,

$$\tilde{\boldsymbol{Z}}\boldsymbol{X} = \tilde{\boldsymbol{Y}}, \quad (9)$$

where $\tilde{\boldsymbol{Z}} = \boldsymbol{R}_1\boldsymbol{Z}$, $\tilde{\boldsymbol{Y}} = \boldsymbol{R}_1\boldsymbol{Y}$, and

$$\boldsymbol{R}_1 = \begin{bmatrix} \boldsymbol{I} & \boldsymbol{R}_{12} & \boldsymbol{R}_{13} & \boldsymbol{O} & \boldsymbol{O} & \boldsymbol{O} \\ \boldsymbol{O} & \boldsymbol{I} & \boldsymbol{O} & \boldsymbol{O} & \boldsymbol{O} & \boldsymbol{O} \\ \boldsymbol{O} & \boldsymbol{O} & \boldsymbol{I} & \boldsymbol{O} & \boldsymbol{O} & \boldsymbol{O} \\ \vdots & \vdots & \vdots & \vdots & \vdots & \vdots \\ \boldsymbol{O} & \boldsymbol{O} & \boldsymbol{O} & \boldsymbol{O} & \cdots & \boldsymbol{I} \end{bmatrix}. \quad (10)$$

$\boldsymbol{R}_{12}$ and $\boldsymbol{R}_{13}$ are $M \times M$ matrices with unknown coefficients, and $\boldsymbol{I}$ and $\boldsymbol{O}$ are $M \times M$ identity and null matrices, respectively.

Considering the first row of the $\tilde{\boldsymbol{Z}}$-matrix, we have:

$$\begin{aligned} \tilde{\boldsymbol{Z}}_{11} &= \boldsymbol{Z}_{11} + \boldsymbol{R}_{12}\boldsymbol{Z}_{21} + \boldsymbol{R}_{13}\boldsymbol{Z}_{31} \\ \tilde{\boldsymbol{Z}}_{12} &= \boldsymbol{Z}_{12} + \boldsymbol{R}_{12}\boldsymbol{Z}_{22} + \boldsymbol{R}_{13}\boldsymbol{Z}_{32} \\ \tilde{\boldsymbol{Z}}_{13} &= \boldsymbol{Z}_{13} + \boldsymbol{R}_{12}\boldsymbol{Z}_{23} + \boldsymbol{R}_{13}\boldsymbol{Z}_{33} \\ &\vdots \quad \vdots \quad \vdots \\ \tilde{\boldsymbol{Z}}_{1P} &= \boldsymbol{Z}_{1P} + \boldsymbol{R}_{12}\boldsymbol{Z}_{2P} + \boldsymbol{R}_{13}\boldsymbol{Z}_{3P}. \end{aligned}$$

Next, we solve for $\boldsymbol{R}_{12}$ and $\boldsymbol{R}_{13}$ by forcing the elements of $\tilde{\boldsymbol{Z}}_{12}$ and $\tilde{\boldsymbol{Z}}_{13}$ to zero. Thus, we solve

$$\begin{aligned} \boldsymbol{Z}_{12} + \boldsymbol{R}_{12}\boldsymbol{Z}_{22} + \boldsymbol{R}_{13}\boldsymbol{Z}_{32} &= 0, \quad (11) \\ \boldsymbol{Z}_{13} + \boldsymbol{R}_{12}\boldsymbol{Z}_{23} + \boldsymbol{R}_{13}\boldsymbol{Z}_{33} &= 0, \quad (12) \end{aligned}$$

simultaneously, which results in a solution of $2M \times 2M$ matrix with M right hand sides. Once, $\boldsymbol{R}_{12}$ and $\boldsymbol{R}_{13}$ are known, it is trivial to obtain $\tilde{\boldsymbol{Y}}$. Note that the procedure described so far sets the interaction between groups 1 and 2 ($\tilde{\boldsymbol{Z}}_{12}$) and between groups 1 and 3 ($\tilde{\boldsymbol{Z}}_{13}$) to zero and makes $\tilde{\boldsymbol{Z}}_{11}$ dominant block in the row.

By applying a similar procedure to rows $2, 3, \cdots, P$ and each time solving a $2M \times 2M$ matrix, we can generate a new matrix equation, given by,

$$\overline{\boldsymbol{Z}}\boldsymbol{X} = \overline{\boldsymbol{Y}}, \quad (13)$$

where the new $\overline{\boldsymbol{Z}}$-matrix is given by

$$\begin{bmatrix} \tilde{\boldsymbol{Z}}_{11} & \boldsymbol{O} & \boldsymbol{O} & \cdots & \tilde{\boldsymbol{Z}}_{1,P-2} & \tilde{\boldsymbol{Z}}_{1,P-1} & \tilde{\boldsymbol{Z}}_{1P} \\ \boldsymbol{O} & \tilde{\boldsymbol{Z}}_{22} & \boldsymbol{O} & \cdots & \tilde{\boldsymbol{Z}}_{2,P-2} & \tilde{\boldsymbol{Z}}_{2,P-1} & \tilde{\boldsymbol{Z}}_{2P} \\ \tilde{\boldsymbol{Z}}_{31} & \boldsymbol{O} & \tilde{\boldsymbol{Z}}_{33} & \cdots & \tilde{\boldsymbol{Z}}_{3,P-2} & \tilde{\boldsymbol{Z}}_{3,P-1} & \tilde{\boldsymbol{Z}}_{3P} \\ \vdots & \vdots & \vdots & \vdots & \vdots & \vdots & \vdots \\ \tilde{\boldsymbol{Z}}_{P1} & \tilde{\boldsymbol{Z}}_{P2} & \tilde{\boldsymbol{Z}}_{P3} & \cdots & \boldsymbol{O} & \boldsymbol{O} & \tilde{\boldsymbol{Z}}_{PP} \end{bmatrix}$$

and

$$\overline{\boldsymbol{Y}} = \left[\tilde{\boldsymbol{Y}}_1, \tilde{\boldsymbol{Y}}_2, \tilde{\boldsymbol{Y}}_3, \tilde{\boldsymbol{Y}}_4, \cdots, \tilde{\boldsymbol{Y}}_P\right]^T.$$

We note that the $\overline{\boldsymbol{Z}}$-matrix in Eq. (13) represents a diagonally-dominant matrix assuming sufficient number of basis functions are collected in a group.

Next, let $\overline{\boldsymbol{Z}} = \overline{\boldsymbol{Z}}_d + \overline{\boldsymbol{Z}}_{off}$ where $\overline{\boldsymbol{Z}}_d$ includes only diagonal blocks of the $\overline{\boldsymbol{Z}}$-matrix and $\overline{\boldsymbol{Z}}_{off}$-matrix includes the remaining blocks. We now have,

$$\begin{aligned} \left[\overline{\boldsymbol{Z}}_d + \overline{\boldsymbol{Z}}_{off}\right]\boldsymbol{X} &= \overline{\boldsymbol{Y}} \\ \Rightarrow \overline{\boldsymbol{Z}}_d\left[\boldsymbol{I} + \overline{\boldsymbol{Z}}_d^{-1}\overline{\boldsymbol{Z}}_{off}\right]\boldsymbol{X} &= \overline{\boldsymbol{Y}} \\ \Rightarrow \left[\boldsymbol{I} + \overline{\boldsymbol{Z}}_d^{-1}\overline{\boldsymbol{Z}}_{off}\right]\boldsymbol{X} &= \overline{\boldsymbol{Z}}_d^{-1}\overline{\boldsymbol{Y}} \\ \Rightarrow \left[\boldsymbol{I} + \boldsymbol{U}\right]\boldsymbol{X} &= \boldsymbol{X}_0. \quad (14) \end{aligned}$$

In Eq. (14), $\boldsymbol{X}_0 = \overline{\boldsymbol{Z}}_d^{-1}\overline{\boldsymbol{Y}}$ and $\boldsymbol{U} = \overline{\boldsymbol{Z}}_d^{-1}\overline{\boldsymbol{Z}}_{off}$.

Finally, the solution $\boldsymbol{X}$ may be obtained by expanding Eq. (14) in power series as,

$$\begin{aligned} \boldsymbol{X} &= \left[\boldsymbol{I} + \boldsymbol{U}\right]^{-1}\boldsymbol{X}_0 \\ &= \left[\boldsymbol{I} - \boldsymbol{U} + \boldsymbol{U}^2 - \boldsymbol{U}^3 + \cdots\right]\boldsymbol{X}_0 \\ &= \boldsymbol{X}_0 - \boldsymbol{U}\boldsymbol{X}_0 + \boldsymbol{U}[\boldsymbol{U}\boldsymbol{X}_0] \\ &\quad -\boldsymbol{U}(\boldsymbol{U}[\boldsymbol{U}\boldsymbol{X}_0]) + \cdots. \quad (15) \end{aligned}$$

The necessary and sufficient condition for the power series in Eq. (15) to converge is the Frobenius norm [10] $||\boldsymbol{U}|| \leq 1$. To achieve this condition, it may be easier to enforce $||\overline{\boldsymbol{Z}}_d^{-1}|| \cdot ||\overline{\boldsymbol{Z}}_{off}|| \leq 1$. The norms of $\overline{\boldsymbol{Z}}_d^{-1}$ and $\overline{\boldsymbol{Z}}_{off}$ can be easily computed while generating these terms and ensure that the necessary condition is satisfied. Alternatively, one may adopt the following procedure.

We note that,

$$\begin{aligned} ||\overline{\boldsymbol{Z}}_d^{-1}|| &= \frac{||\overline{\boldsymbol{Z}}_d^{-1}|| \cdot ||\overline{\boldsymbol{Z}}_d\boldsymbol{X}_0||}{||\overline{\boldsymbol{Z}}_d\boldsymbol{X}_0||} \\ &\leq \frac{||\overline{\boldsymbol{Z}}_d^{-1}|| \cdot ||\overline{\boldsymbol{Z}}_d|| \cdot ||\boldsymbol{X}_0||}{||\overline{\boldsymbol{Y}}||} \\ &= \kappa_d\frac{||\boldsymbol{X}_0||}{||\overline{\boldsymbol{Y}}||}, \quad (16) \end{aligned}$$

where $\kappa_d = ||\overline{\boldsymbol{Z}}_d^{-1}|| \cdot ||\overline{\boldsymbol{Z}}_d||$ represents the condition number of $\overline{\boldsymbol{Z}}_d$.

Next, we define $\overline{\boldsymbol{Y}}_e = \overline{\boldsymbol{Z}}\boldsymbol{X}_0 - \overline{\boldsymbol{Z}}_d\boldsymbol{X}_0 = \overline{\boldsymbol{Z}}_{off}\boldsymbol{X}_0$ and we have,

$$\begin{aligned} ||\overline{\boldsymbol{Z}}_{off}|| &= \frac{||\overline{\boldsymbol{Z}}_{off}|| \cdot ||\overline{\boldsymbol{Z}}_{off}^{-1}\overline{\boldsymbol{Y}}_e||}{||\overline{\boldsymbol{Z}}_{off}^{-1}\overline{\boldsymbol{Y}}_e||} \\ &\leq \frac{||\overline{\boldsymbol{Z}}_{off}|| \cdot ||\overline{\boldsymbol{Z}}_{off}^{-1}|| \cdot ||\overline{\boldsymbol{Y}}_e||}{||\boldsymbol{X}_0||} \\ &= \kappa_{off}\frac{||\overline{\boldsymbol{Y}}_e||}{||\boldsymbol{X}_0||}, \end{aligned} \tag{17}$$

where $\kappa_{off} = ||\overline{\boldsymbol{Z}}_{off}^{-1}|| \cdot ||\overline{\boldsymbol{Z}}_{off}||$ represents the condition number of $\overline{\boldsymbol{Z}}_{off}$.

Combining Eqs. (16) and (17), we have,

$$||\overline{\boldsymbol{Z}}_d^{-1}|| \cdot ||\overline{\boldsymbol{Z}}_{off}|| \leq \kappa_d\kappa_{off}\frac{||\overline{\boldsymbol{Y}}_e||}{||\overline{\boldsymbol{Y}}||} \tag{18}$$

and, to satisfy the condition $||\boldsymbol{U}|| \leq 1$, we must ensure that

$$\frac{||\overline{\boldsymbol{Y}}_e||}{||\overline{\boldsymbol{Y}}||} \leq \frac{1}{\kappa_d\kappa_{off}}. \tag{19}$$

We note that, it is not really necessary to compute the condition numbers κ_d and κ_{off} but ensure that the fraction $\frac{||\overline{\boldsymbol{Y}}_e||}{||\overline{\boldsymbol{Y}}||}$ is a small number. Our various numerical experiments suggested that this number must be less than 0.4. It is because the described numerical implementation ensures that matrices $\overline{\boldsymbol{Z}}_d$ and $\overline{\boldsymbol{Z}}_{off}$ are well-conditioned matrices. Obviously, if the $\frac{||\overline{\boldsymbol{Y}}_e||}{||\overline{\boldsymbol{Y}}||}$ is not less than the empirical value then the solution may diverge and the procedure needs to be reimplemented by increasing the group size.

Alternatively, it is also possible to solve Eq. (13) by carrying out the following mathematical and numerical operations:

1. Obtain $\boldsymbol{X}_0$ as before by solving the equation $\overline{\boldsymbol{Z}}_d\boldsymbol{X}_0 = \overline{\boldsymbol{Y}}$.
2. Obtain $\overline{\boldsymbol{Y}}_0$ by performing $\overline{\boldsymbol{Y}}_0 = \overline{\boldsymbol{Z}}\boldsymbol{X}_0$. Then, we have $\overline{\boldsymbol{Z}}\boldsymbol{X} = \overline{\boldsymbol{Y}}$ and $\overline{\boldsymbol{Z}}\boldsymbol{X}_0 = \overline{\boldsymbol{Y}}_0$.
3. Thus, we have $\overline{\boldsymbol{Z}}(\boldsymbol{X} - \boldsymbol{X}_0) = (\overline{\boldsymbol{Y}} - \overline{\boldsymbol{Y}}_0)$, which is in the same form as Eq. (13). Hence, the process can be repeated till we have convergence. Note that, for the iterative process to converge, we must satisfy Eq. (19).

III. IMPLEMENTATION, GUIDELINES, AND OBSERVATIONS

The procedure developed so far can be applied to any MOM problem involving PEC bodies. Assuming that we have an electrically large problem to solve, we present a few important pointers to develop the solution in an efficient manner:

- **Implementation**
  - **Symmetric matrix** - We note that the procedure described so far uses same functions for expansion and testing resulting in Galerkin procedure and symmetric $\boldsymbol{Z}$-matrix. However, it is common to use approximations in the testing procedure thus destroying the symmetry property [9]. This problem can be easily remedied by taking the average of Z_{ij} and Z_{ji} for $j = 1, 2, \cdots, N$ and $i = 1, 2, \cdots, j$. This procedure is fairly common and, given reasonable number of unknowns for the problem, does not result in loss of accuracy [9]. In fact, many commercial algorithms prefer this approach to take advantage of the symmetric matrix and thereby reducing the storage requirements.
  - **Sorting the basis functions** - The algorithm requires that the basis functions be ordered according to distance measured from a reference point. The placement of the reference point is not critical. It may be placed at one end or just outside the structure. It is quite easy to measure the distance to the center of each basis function i.e., to the center of the linear segment (edge) for two (three) dimensional problems. Then, one may use any efficient sorting algorithm to order the basis functions.
  - **Generating groups** - The geometry of the problem is divided up into disjoint groups. One way of obtaining the number of groups is to select a reasonable group size, i.e., number of basis functions in the group, and divide the total number of basis functions by the group size. It is important to note that a relatively few number of basis functions in a group would cause the solution to diverge. Hence, it is recommended to make the group division using distance criterion such as 0-10λ in the first group, 10-20λ in the second group, and so on for two dimensional problems, assuming the reference point is the center of the first basis function. For three dimensional problems, the guide lines are 0-3λ in the first group, 3-6λ in the second group, and so on. Further, it is also recommended that one would be better off by choosing as many number of basis functions in a group as possible since it would make the power series solution to converge faster.

  - **Storage requirements** - Note that it is efficient to store only the diagonal blocks of the $\overline{\boldsymbol{Z}}$-matrix and the coefficient matrices. Thus, the storage required is $P*M^2 = N*M$ for diagonal blocks and $2P*M^2 = 2N*M$ for coefficient matrices. The $\boldsymbol{U}$-matrix is not stored and computed as needed since only a couple terms in the power series are needed for accurate solution. Thus, the total required storage is $3N*M$.

- **Guidelines**
  - It is necessary, convenient, and hence, recommended to perform sorting and grouping before beginning the electromagnetic solution. However, this only needs to be done once.
  - One may develop a simple algorithm to develop the diagonal blocks of $\overline{\boldsymbol{Z}}$-matrix and may be performed either serially or in parallel. Obviously, parallel solution reduces the computation time drastically and one can achieve almost linear efficiency with the number of processors since computation of each block is independent from another block.
  - If a sufficient number of basis functions are assembled into a group, only a few terms are required in the power series solution. Generally, one or two terms are sufficient for accurate solution. For very large problems involving several hundred thousand unknowns, it is recommended to use as much a large group matrix as possible. For such cases, even one term in the power series may be sufficient. It is cautioned that an insufficiently smaller group size may require large number of terms in the power series to converge and may even diverge.

- **Observations**
  - We observe that, although the numerical procedure presented in this work is a substantial improvement to [8], the remarks concerning the usage of CPU time, parallel processing, and efficiency are also applicable for the present work. Further, this procedure eliminates several time consuming steps and hence results in higher efficiency. In Table 1, we present the actual elapsed CPU time, in seconds, for conventional MOM procedure and power series procedure. The computer used for this purpose is Intel Core2 computer at 2.66 GHz clock speed running a single thread. We note that the computational times in this work follow $\bigcirc(N^2)$ trend.

Table 1: The elapsed tine in seconds as a function of unknowns

No. of Unknowns	MOM	Power Series
792	3.04	4.72
2,997	45	34
6,270	410	294
8,355	916.18	441
13,500	3,662	1,645
25,080	22, 353	5,204
53,856	147,600	27,720

  - Since this procedure is designed to handle electrically large problems, one may be able to judiciously vary the order of integration depending upon the location of source and field points.
  - We observe that the procedure presented in this work is more amenable for parallel processing as compared to the conventional MOM. To illustrate this point, we present an almost linear scaling of the CPU time with number of processors as shown in Fig. 1. Note that a ship like object modeled with 216,000 basis functions and a group size of 1400 is used for generating this data.

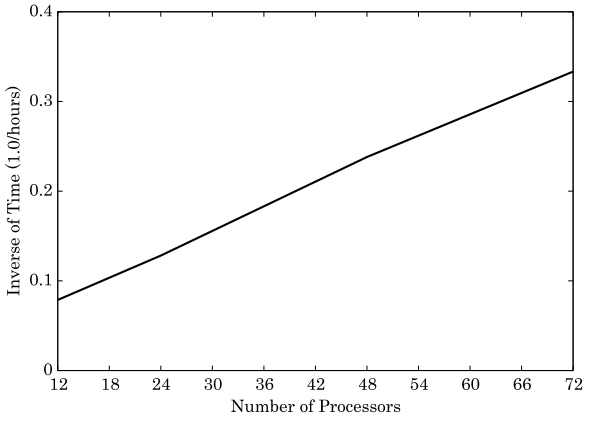

Fig. 1. Inverse of elapsed time as a function of number of processors.

IV. NUMERICAL RESULTS

In this section, we present a few representative numerical results involving both two- and three-dimensional bodies for validation purposes. We present the bistatic/monostatic radar cross section (RCS) calculations of several objects and compare either with the standard method of moments solution or exact solution where available. We note that the current distribution is also checked and found to be of the same level of accuracy as the RCS for all the

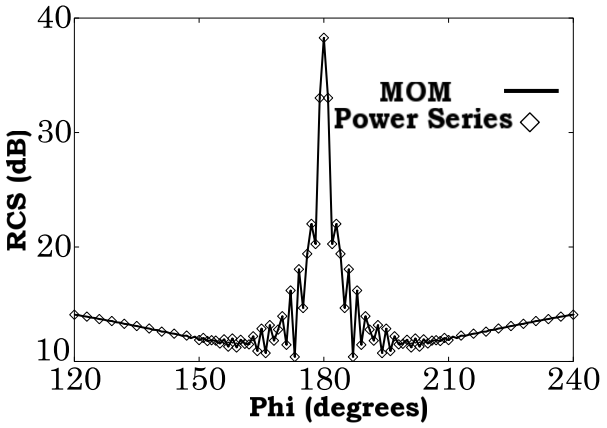

Fig. 2. RCS of a two-dimensional conducting cir-cular cylinder of 100λ circumference illuminated by a TM wave.

representative examples even though we present current distribution on a three-dimensional finite cylinder case only for the sake of completeness. Further, for all the results presented in this section, only two terms are used in the power series solution.

The first example is a two-dimensional circular cylinder with a perimeter=100λ illuminated by a transverse magnetic (TM) plane wave. The circumference of the cylinder is divided into 1000 linear segments. Figure 2 shows the bistatic RCS as a function of the azimuthal angle ϕ. We compare the results of the present method with the standard MOM solution. For the present solution, the total number of basis functions has been grouped into 5 groups. The comparison is excellent between these two procedures.

The next example is a two-dimensional square cylinder, side length=50λ, illuminated by TM plane wave as shown in the inset of Fig. 3. The square cross section is approximated by 2,000 unknowns for MOM solution. For the present method, the group size is 200 with 10 groups in total. We present the

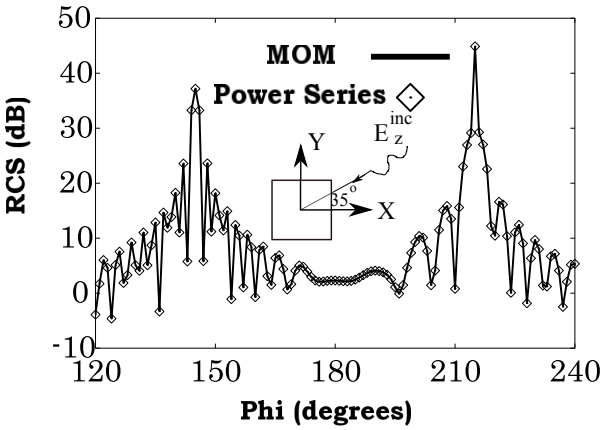

Fig. 3. RCS of a two-dimensional square cylinder of 200λ circumference illuminated by a TM wave.

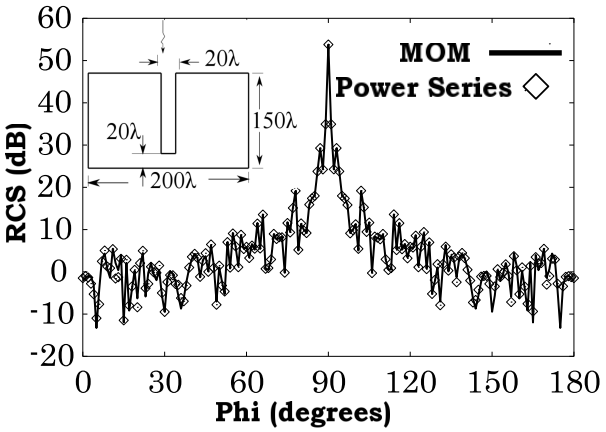

Fig. 4. RCS of a two-dimensional complex cross-section cylinder of 960λ circumference illuminated by a TM wave.

bistatic RCS as a function of the azimuthal angle ϕ and compare with MOM solution as shown in Fig. 3. The comparison is excellent for this example also.

As a third example, we consider a two dimensional cylinder with complex cross section illuminated by TM plane wave as shown in the inset Fig. 4. The total circumference of the cylinder is 960λ, approximated by 9,600 unknowns, and divided into 5 groups for the present solution. Figure 4 shows the bistatic RCS compared as a function of the azimuthal angle ϕ to the MOM solution.

Next, we present the case of a large circular cylinder with a circumference of 100,000λ. The circumference is approximated by one million unknowns and divided into 1000 groups. Once again, only two terms in the power series solution is used. The RCS for this case is shown in Fig. 5. Although no comparison is shown here, this case is presented to highlight the capability of the present method to easily handle very large problems.

Next, we consider three-dimensional problems.

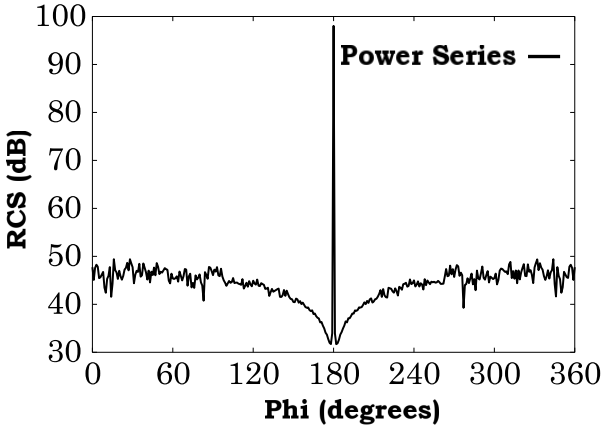

Fig. 5. RCS of a two-dimensional conducting cir-cular cylinder of 100, 000λ circumference illuminated by a TM wave.

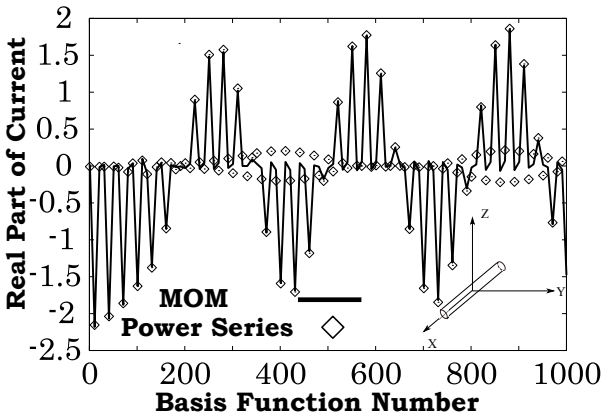

Fig. 6. Real part of the current distribution on a three-dimensional conducting cylinder, $L = 20\lambda$ and radius $a = 0.318\lambda$, placed along the x-axis illuminated by a x-polarized, z-traveling plane wave.

Consider a long conducting cylinder, $L = 20\lambda$ and radius $a = 0.318\lambda$, closed at both ends.The cylinder is placed along the x-axis and illuminated by a x-polarized plane wave traveling along the z-axis. The cylinder is approximated by 6270 RWG basis functions. For the present solution method, the total number of basis functions are divided into 10 groups with each group consisting 627 basis functions. In Fig. 6, we present the real part of the induced current as a function of basis function numbers. Note that only a part of the figure, i.e., basis functions from 1 to 1000, is presented for the sake of clarity. The bistatic RCS for this case is shown in the Fig. 7 and compared with the MOM solution. We note a good comparison of the present method with MOM solution for both current distribution and RCS. Although not presented here, the imaginary part of the current shows similar level of comparison.

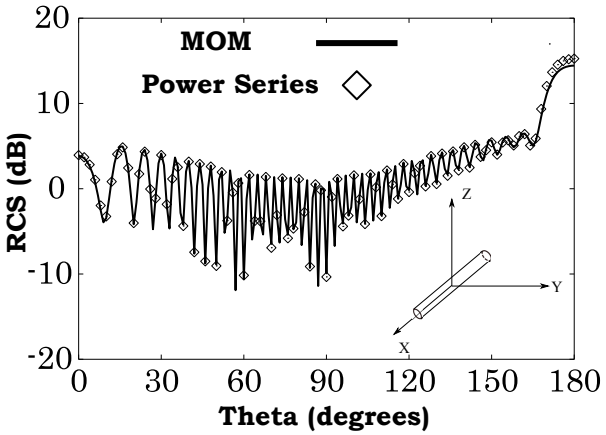

Fig. 7. RCS of a three-dimensional conducting cylinder, $L = 20\lambda$ and radius $a = 0.318\lambda$, placed along the x-axis illuminated by a x-polarized, z-traveling plane wave.

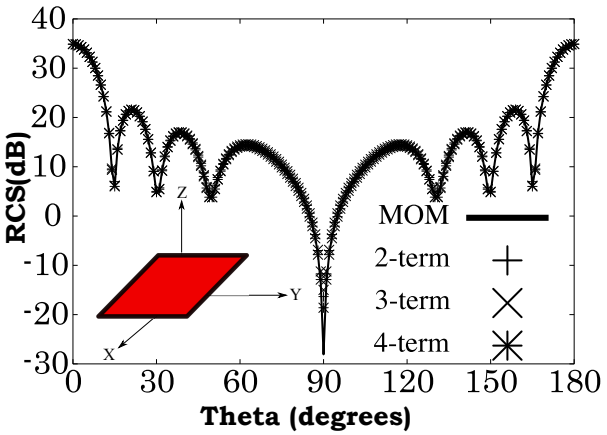

Fig. 8. RCS of a three-dimensional conducting square plate, $L = 4\lambda$, placed along the xy-plane il-luminated by a x-polarized, z-traveling plane wave.

Next, consider a 4λ square plate placed in the xy-plane and illuminated by a x-polarized plane wave traveling along the z-axis. The plate is approximated by 5,000 triangles resulting in 7,400 basis functions. For the present solution method, the total number of basis functions are divided into 10 groups with each group consisting of 740 basis functions. The bistatic RCS for this case is shown in the Fig. 8 and compared with the MOM solution. The comparison of the present method with MOM solution is again very good except at $\theta = 90^0$ where the MOM procedure presents a deeper null. For this example, we added more terms in the power series to show the convergence of the procedure. It is noted that after two terms, the results did not change appreciably except at the null region.

Next, we consider two conducting spheres, with radii of 3.0λ and and 5.0λ illuminated by a x-polarized plane wave traveling along the z-axis. The

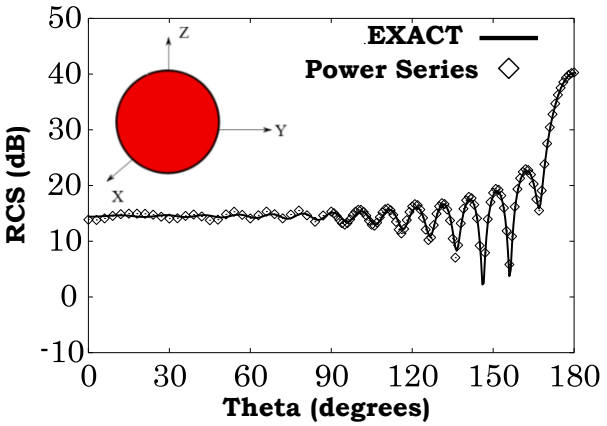

Fig. 9. RCS of a three-dimensional conducting sphere, radius $a = 3\lambda$, placed with center coinciding with the origin and illuminated by a x-polarized, z-traveling plane wave. Number of unknowns=29,400. Number of groups=50.

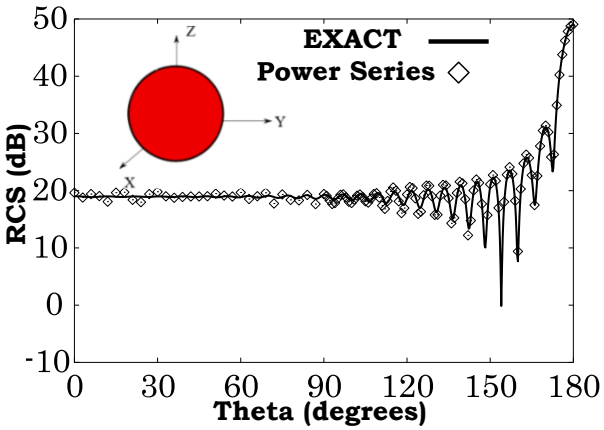

Fig. 10. RCS of a three-dimensional conducting sphere, radius $a = 5\lambda$, placed with center coinciding with the origin and illuminated by a x-polarized, z-traveling plane wave. Number of unknowns=93,750. Number of groups=125.

spheres are approximated by 29,400 and 93,750 basis functions, respectively. The group size for the 3.0λ case is 588 implying 50 groups in total. Similarly, the group size for the 5.0λ case is 750 and a total of 125 groups. The bistatic RCS for these two cases is shown in the Figs. 9 and 10, respectively and compared with exact Mie series [11] solution. We note a reasonably good comparison for each example with only two terms in the power series.

Now, we consider more complex, non-canonical objects to illustrate the usefulness of the proposed method. Consider an aircraft-type model illuminated by a x-polarized plane wave traveling along the z-axis. The object is located in the XY-plane

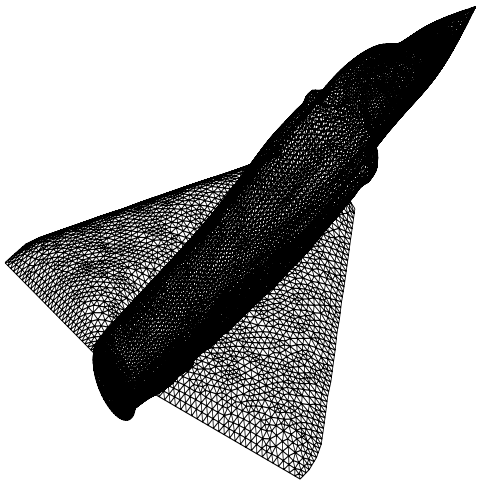

Fig. 11. Triangulated model of an aircraft.

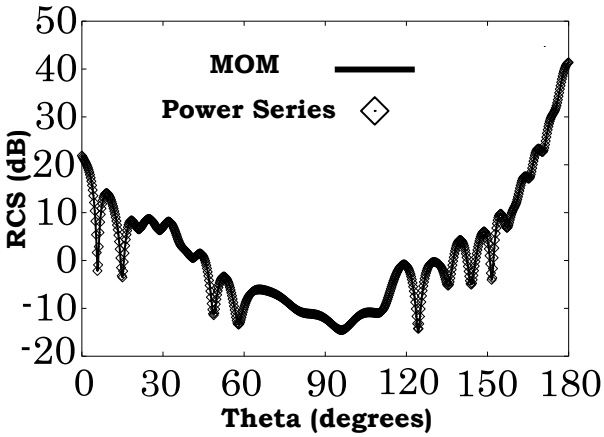

Fig. 12. RCS of an aircraft-type object. Number of unknowns=25,080. Number of groups=12.

with nose along the x-axis. The largest dimensions of the aircraft along x, y and z directions are 11.6λ, 9.2λ, and 1.6λ, respectively. The aircraft is approximated by 25,080 basis functions as shown in Fig. 11. For the power series solution, the total number of basis functions is divided into 12 groups with 2090 basis functions in each group. The bistatic RCS along XZ-plane is shown in Fig. 12. The power series solution is compared with MOM solution and we note a reasonably good comparison for this complex structure.

Next, we consider a 91 meter ship-like object illuminated by a 100 MHz, x-polarized plane wave traveling along the z-axis. The width and length of the object is along the x and y-axis, respectively. The largest dimensions of the ship-like object along x, y and z directions are 7.5m, 91.5m and 12.4m, respectively. The ship-like object is approximated by 53,832 basis functions as shown in the inset of Fig. 13. For the power series solution, the total number of basis functions is divided into 20 groups with

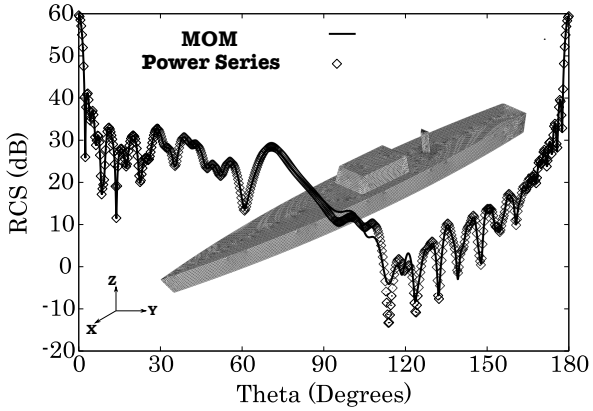

Fig. 13. Bistatic RCS of a 91 m ship-type object at 100 MHz. Number of unknowns=53,856. Number of groups=20.

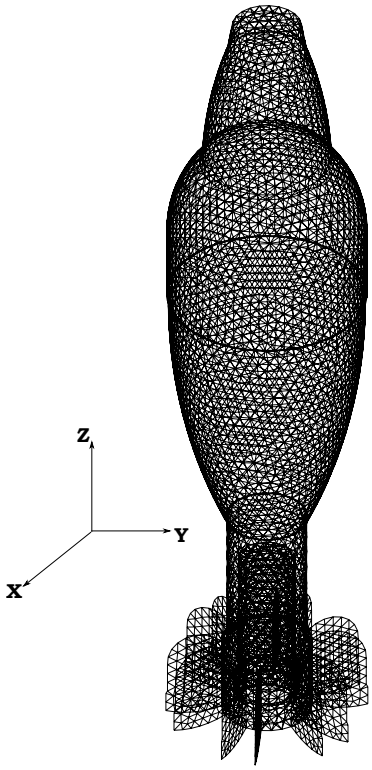

Fig. 14. Triangulated model of a cylindrical-shaped object.

2693 basis functions in each group. The bistatic RCS along YZ-plane is shown in Fig. 13. The power series solution is compared with MOM solution and we note an excellent comparison for this complex structure.

Next, we present a few examples to illustrate the ability of the present work to accurately predict the monostatic radar cross-section. Consider a complex

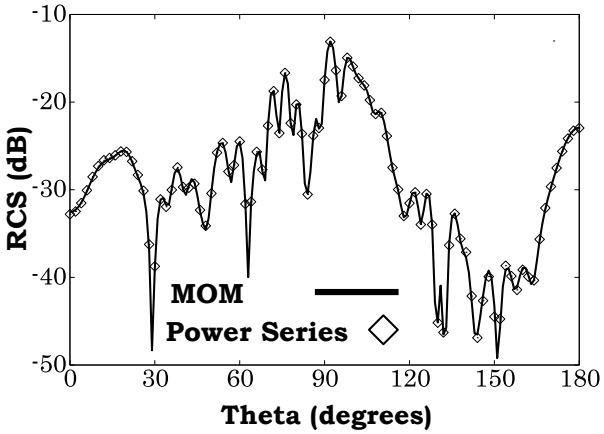

Fig. 15. Monostatic RCS of a cylindrical-shaped object shown in Fig. 14. Number of unknowns=13,010. Number of groups=10.

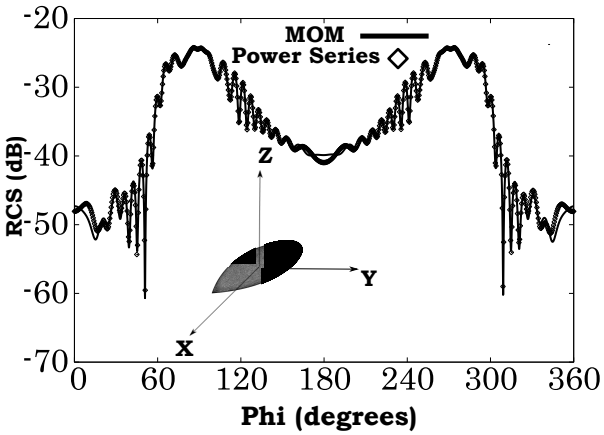

Fig. 16. Monostatic RCS of NASA Almond at 10 GHz. Number of unknowns=46,680. Number of groups=20.

cylindrical-shaped object as shown in the Fig. 14. The height of the object is 105 mm and is cylindrically symmetric along the z-axis. The object is illuminated by 10 GHz plane wave and approximated with 13010 basis functions. For the power-series method, the total number of basis functions are divided into 10 groups with 1301 functions in each group. We present the mono-static elevation RCS of this object using both the conventional MOM and the power series solution method in Fig. 15 and the comparison is excellent between the two methods.

Next, we consider the azimuthal monostatic RCS of NASA Almond ($252mm \times 98mm \times 32mm$), shown in the inset of Fig. 16, at 10 GHz. The electric field is polarized along the z-axis. The object is approximated with 46,680 basis functions. For the power-series method, the total number of basis functions are divided into 20 groups with 2334 functions in each group. For comparison, we also present the conventional MOM. We note excellent comparison between the two methods.

Next, we calculate the elevation ($\phi = 90^0$-cut) monostatic RCS of ship-type object as shown in the inset of Fig. 17. The dimensions and the place of the object is same as in the bistatic ship-type object case. The ship is illuminated by 100 MHz plane wave and polarized along z-direction (height). The object is approximated by 53,856 basis functions and divided into 20 groups for power series solution. It can be seen that there is good comparison between the MOM solution and the present method.

As a final example, again consider the 91 meter ship-like object as shown in the inset of Fig. 18. The purpose of this example is to demonstrate the capability of the present method to handle electrically large, complex shaped objects using MOM involving around million unknowns. The object is illuminated

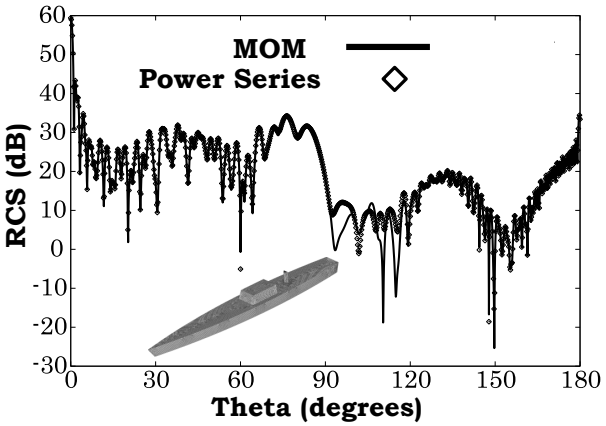

Fig. 17. Monoistatic RCS of a 91m ship-type object at 100 MHz. Number of unknowns=53,856. Number of groups=20.

by a 500 MHz, y-polarized plane wave traveling along the z-axis. To obtain scattering from a higher frequency, the ship is approximated by 864,800 basis functions. For the power series solution, the total number of basis functions is divided into 400 groups with 2162 basis functions in each group. The bistatic RCS along YZ-plane is shown in Fig. 18.

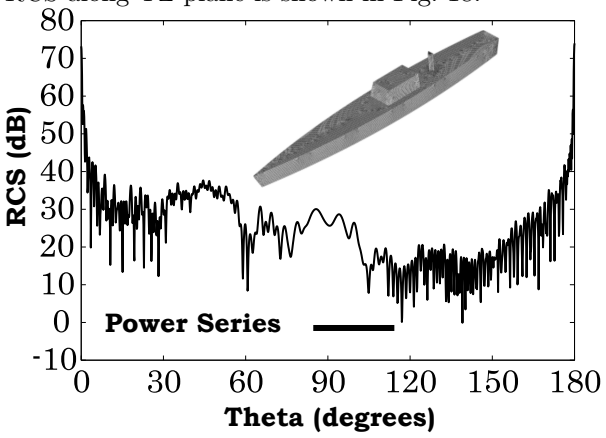

Fig. 18. Bistatic RCS of a 91 m ship-type object a 500 MHz. Number of unknowns=864,800. Number of groups=400.

V. CONCLUSIONS

In this work, we present a new and efficient algorithm to solve the electrically large electromagnetic scattering problems utilizing the MOM formulation. The present method, while handling electrically large PEC bodies, retains all the conventional advantages of MOM, *viz*. accuracy of solution, ability to handle multiple excitation vectors, applicable to scattering and radiation problems, and ability to calculate both near and far-field patterns.The algorithm can be made more efficient using GPU's, more efficient parallel processing, and implementing the adaptive cross approximation (ACA) procedure to reduce the computation of distantly located blocks from the source block [7]. However, some of the aforementioned improvements are not made yet and may be reported in the near future. Lastly, since the method can be viewed as a purely algebraic method, it is envisaged that the method may be applied to any MOM problem with minor modifications.

ACKNOWLEDGEMENTS

This research was conducted under the Naval Research Laboratory Base Program sponsored by the Office of Naval Research. Also, the authors would like to express their appreciation to Dr. Daniel Faircloth, IERUS Technologies, Inc, for providing the input data for Fig. 14.

REFERENCES

[1] R. Harrington, *Field Computation by Moment Methods*, New York, Macmillan, 1968.

[2] E. K. Miller, L. Medgyesi-Mitschang, and E. H. Newman, *Computational Electromagnetics - Frequency-Domain Method of Moments*, IEEE Press, New York, 1992.

[3] W. C. Gibson, *The Method of Moments in Electromagnetics*, Chapman & Hall, Boca Raton, FL, 2008.

[4] T. K. Sarkar, "A note on the choice of weighting functions in the method of moments," *IEEE Transactions on Antennas and Propagation*, vol. 33, pp. 436-441, 1985.

[5] T. K. Sarkar, A. R. Djordjevic, and E. Arvas, "On the choice of expansion and weighting functions in the method of moments," *IEEE Transactions on Antennas and Propagation*, vol. 33, pp. 988-996, 1985.

[6] J. Song, C. C. Lu, and W. C. Chew, "Multilevel fast multipole algorithm for electromagnetic scattering by large complex objects," *IEEE Transactions on Antennas and Propagation*, vol. 45, pp. 1488 - 1493, October 1997.

[7] J. Shaeffer, "Direct solve of electrically large integral equations for problem sizes to 1M unknowns," *IEEE Transactions on Antennas and Propagation*, vol. 56, pp. 2306-2313, 2008.

[8] T. N. Killian, S. M. Rao, and M. E. Baginski, "Electromagnetic scattering from electrically large arbitrarily-shaped conductors using the method of moments and a new null-field generation technique," *IEEE Transactions on Antennas and Propagation*, vol. 59, pp. 537-545, 2011.

[9] S. M. Rao, D. R. Wilton, and A. W. Glisson, "Electromagnetic scattering by surfaces of arbitrary shape," *IEEE Transactions on Antennas and Propagation*, vol. 30, pp. 409-418, 1982.

[10] G. H. Golub and C. F. Van Loan, *Matrix Computations*, 3rd ed. Baltimore, MD: Johns Hopkins, 1996.
[11] R. Harrington, *Time Harmonic Electromagnetic Fields*, New York, IEEE Press, 2001.